Review - experimental study of the MCF processes in solid H/D and H/T mixtures and in gaseous $D/^{3}He$ mixture

Measurement of the pdμ fusion cycle parameters in the solid H/D mixture

M. Filipowicz

- **TRIUMF, Canada**
- **University of Fribourg Switzerland,**
- **PSI (Switzerland),**
- **University of Science and Technology (Poland),**
- **University of California Berkeley (USA),**
- **Institute of Nuclear Physics (Poland)**

JINR, Dubna, Russia

University of British Columbia (Canada),

University of Victoria (Canada),

Gustavus Adolphus College (USA),

Institute for Medium Energy Physics(Wien, Austria)

Processes in solid H/D and H/T mixtures

Interest in investigation of mu-atomic and mu-molecular processes is connected with possibility of obtaining the information about:

- characteristics of nuclear reactions urdergoing in muonic molecules (values of the rates and astrophysical S-factors for these reactions)
- structure of nuclei (measurement of the muonic X rays and Lamb shift of the muonic atom levels)
- efficiencies of the nuclear reactions in muonic molecules (MA and MM processes precede occurence of nuclear fusion reactions in muonic molecules and in this way can determine the muon catalyzed fusion efficiency)
- energy levels of the muonic molecules, what allow to determine effect of the vacuum polarisation
- quantum mechanics problem of the three-body interacting according to Coulomb law is realized

Scattering of muonic atoms

The information about experimental energy dependence of the scattering cross-sections for muonic atoms pμ, dμ and tμ on the hydrogen isotopes molecules

$$p\mu + H_2 \rightarrow p\mu + H_2$$

$$d\mu + H_2 \rightarrow d\mu + H_2$$

$$t\mu + H_2 \rightarrow t\mu + H_2$$

before our measurements practically was absent.

Only estimations of cross-sections for this processes were available, averaged over energy interval of the energy colision 0 - 45 eV.

The knowledge of the cross-section energy dependences is extremelly important becouse MA preceds the muonic molecule formation with following and nuclear fusion in them.

E742 experiment

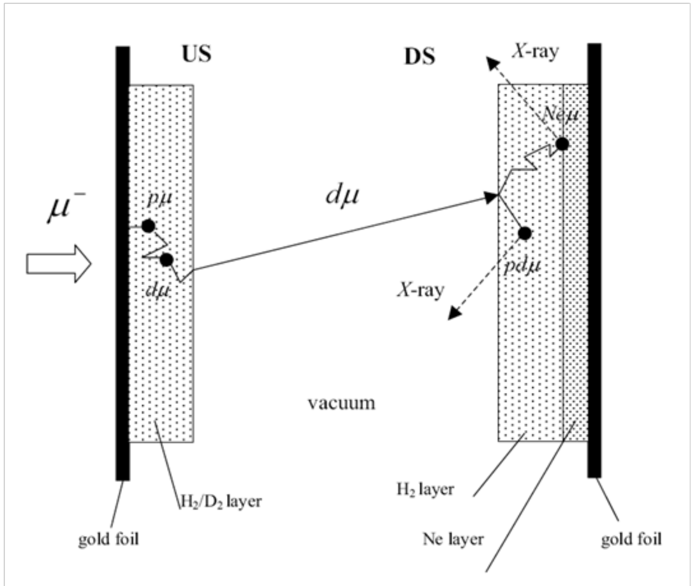

The TOF idea

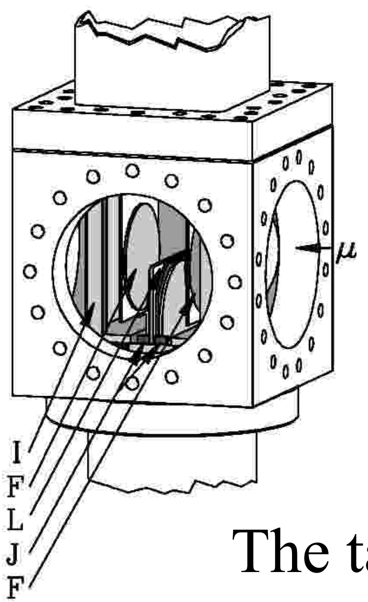

The target system

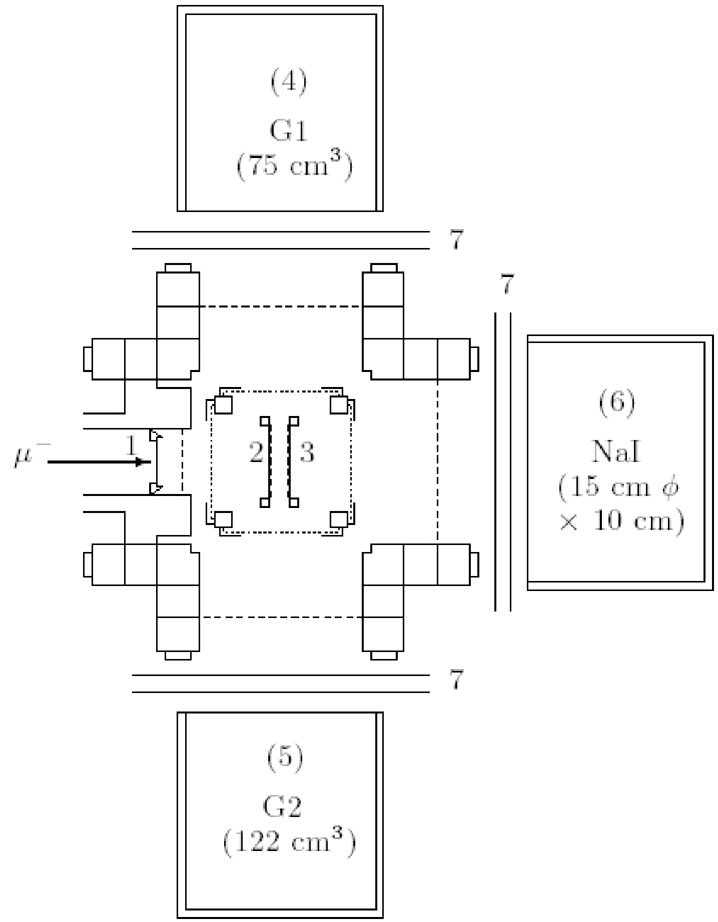

The experimental set-up

Experimental conditions

Label	Experimental purpose	Beam (MeV/c)	US hydrogen (Torr l)	US neon (Torr l)	DS protium (Torr l)	DS neon (Torr l)	GMU (units of 10^6)
D1	RT	26.70	DE			100	326.9
D2	RT	26.70	DE			50	183.3
D3	RT, diff	26.70	DE		300	50	521.8
D4	RT, diff [a]	26.70	DE		600	50	433.2
D5	diff	26.70	DE	100			96.6
D6	diff	26.70	DE	50			136.9
D7	diff	26.70	PP		300	50	149.4
T1	RT	26.25	TE			30	113.5
T2	RT	26.25	TE			50	174.2
T3	RT, diff [a]	26.25	TE		350	50	405.3
T4	RT, diff	26.25	STE		500	50	147.1
T5	diff	26.25	SPP	10			199.3
T6	diff	26.25	SPP	20			195.8

[a]D4 and T3 are not useful for the $p\mu$ diffusion analysis due to the strong overlap between RT and diffusion parts of the time spectra.

Different measurements performed for the RT and $p\mu$ diffusion *(diff)* studies. 1500 Torr l (H_2 + 0.05% D_2) covered with 500-Torr l H_2. DE (deuterium emission). TE (tritium emission)—2000 Torr l (H_2 + 0.12% T_2). STE (small tritium emission)—1000 Torr l (H_2 + 0.12% T_2). PP (pure protium) —2000 Torr l H_2. SPP (small pure protium) — 1000 Torr l H_2. GMU—good muons: i.e., events when only one muon entered the apparatus (no pileup). Conversion factor (for hydrogen): 1 Torr l corresponds to 3.4 μg cm^{-2} for H_2

Main results

- The energy dependence of the scattering cross-section,
- The experimental determination of RT effect characteristics,
- The abnormally high emission of the pμ atoms,
- Experimentally verified that pμ scattering at low energies due to elastic Bragg and phonon scattering – theoretical predicton
- The possibility of generation ultracold pμ atoms
- The characteristics of processes in pdμ and ptμ molecules were found (the formation rate and fusion characteristics)
- The value of astrophysical S-factor was obtained

Publication results

[1] V.M. Bystritsky et al., Proposal E 742 (TRIUMF, Canada) Scattering of muonic hydrogen isotopes - TRIUMF,Canada,1995; V.M.Bystritsky et al., Proposal TRIUMF E 742 – Progress Report 1996.

[2] R. Jacot-Guillarmod,... V.M. Bystritsky et al., Investigation of muonic hydrogen isotopes scattering from H2 molecules, Hyp. Interaction 101/102 (1996) 563-571.

[3] J.Wozniak, ... V.M. Bystritsky et al., Study of muonic hydrogen transport in TRIUMF experiment E 742 by Monte Carlo Method, Hyp. Interaction 101/102 (1996) 573-582.

[4] F.Mulhauser,.. V.M. Bystritsky et al., Scattering of Muonic Hydrogen Atoms, Hyp. Interactions 118 (1999) 35-44.

[5] J.Wozniak, .. V.M. Bystritsky et al., New effects in low energy scattering of $p\mu$ atoms, Hyp. Interactions 119 (1999) 63-70.

[6] A. Olin,...V.M. Bystritsky et al., Study of μ-catalyzed fusion in H-D mixtures, Hyp. Interactions 118 (1999) 163-170.

[7] F.Mulhauser,.... V.M. Bystritsky et al., Ramsauer-Townsend effect in solid hydrogen, Hyp. Interaction 138 (2002) 41-46.

[8] V.M. Bystritsky et al., Generation of the Ultralow Muonic Hydrogen Flux, Hyp. Interaction 138 (2002) 47-53.

[9] G. Marshall,... V.M. Bystritsky et al., Advantages and limitations of solid layer experiments in muon catalyzed fusion, Hyp. Interaction 138 (2002) 203-211.

[10] V.M. Bystritsky et al., Method of Determination of Muon Catalyzed Fusion Parameters in H-T, European Phys. Journal D 26 (2003) 131-139.

[11] M. Filipowicz,.... V.M. Bystritsky et al., Method of Monte Carlo grid for data analysis, Nucl. Instrum. And Meth. A547 (2005) 652 - 662.

[12] J. Wozniak,... V.M. Bystritsky et al., Scattering of $p\mu$ muonic atoms in solid hydrogen, Phys. Rev. A 68 (2004) 062502

The RT effects origin and its study

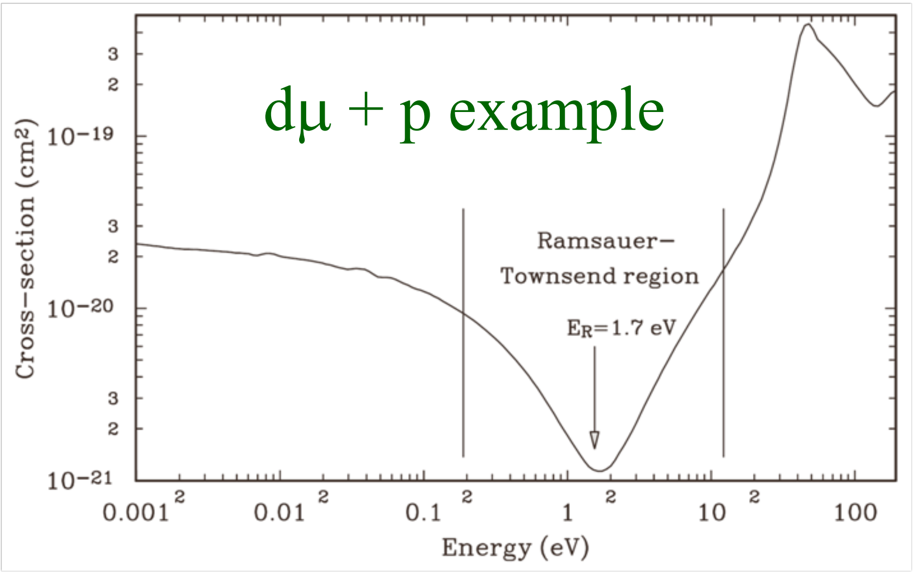

Example of the cross-section parametrisation (shift) and the parametrised time spectra

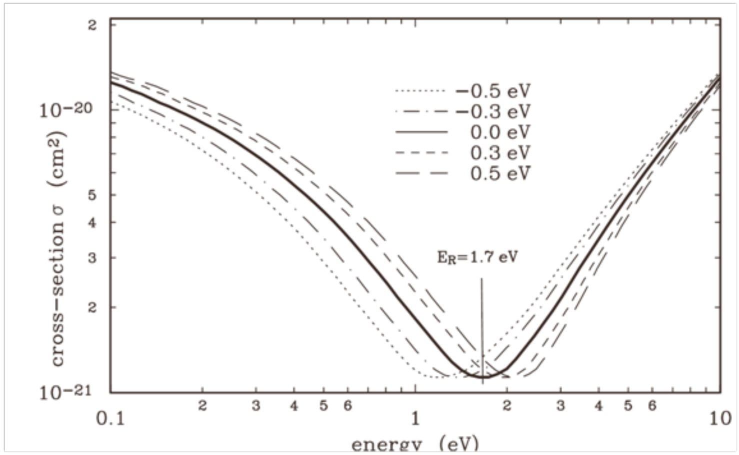

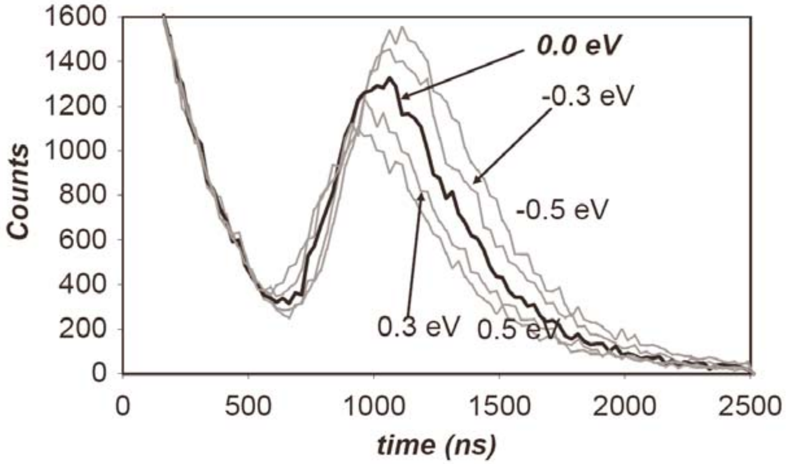

Abnormally high pμ emission and RT effect

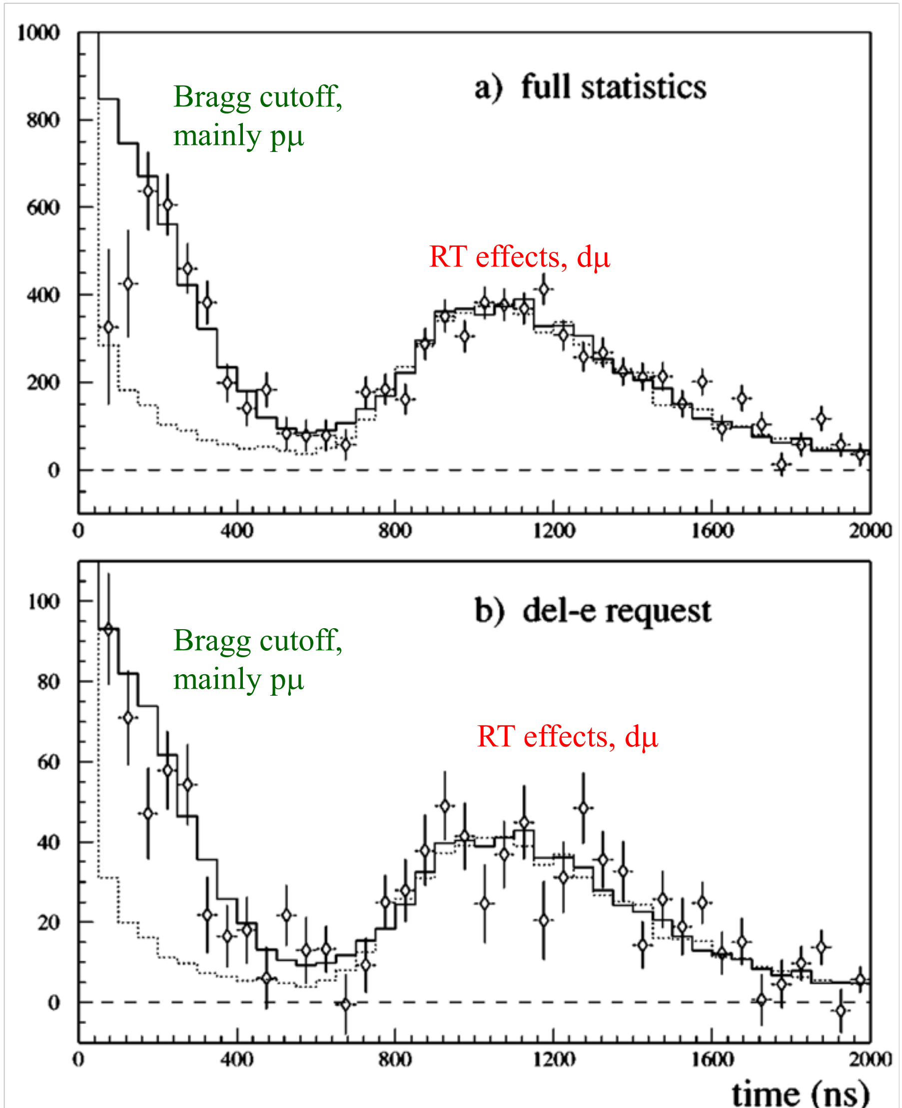

Experimental time-of-flight spectra (points with error bars) for example experiment for cases:

a) full statistics,

b) del-*e* criteria.

The solid line represents the Monte Carlo simulation based on the scattering cross sections when solid effects were taken into account, the dotted line is for the gas cross sections.

The abormally high pμ emission is visible

The Bragg cut-off

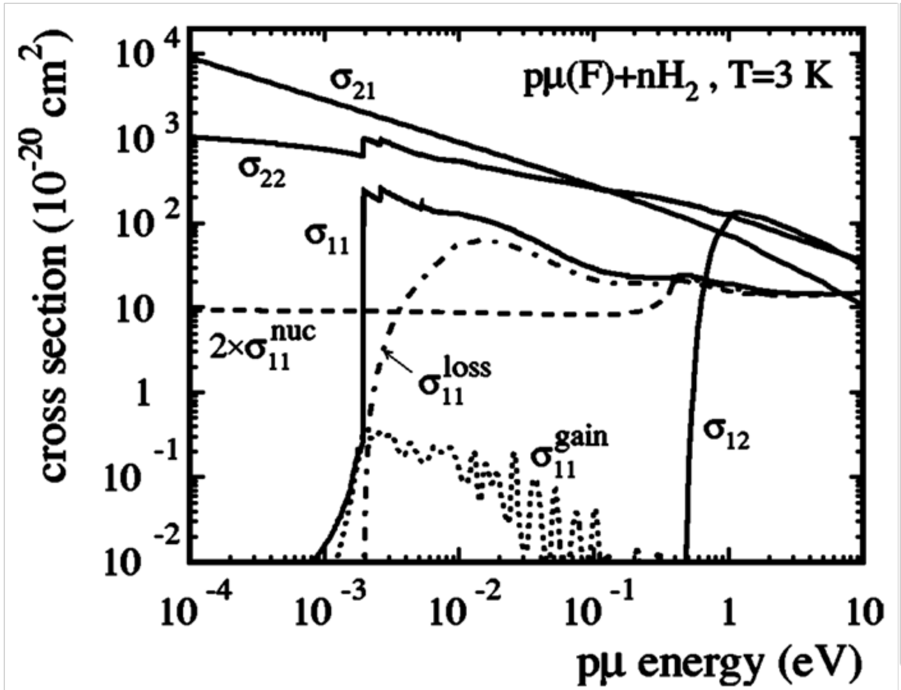

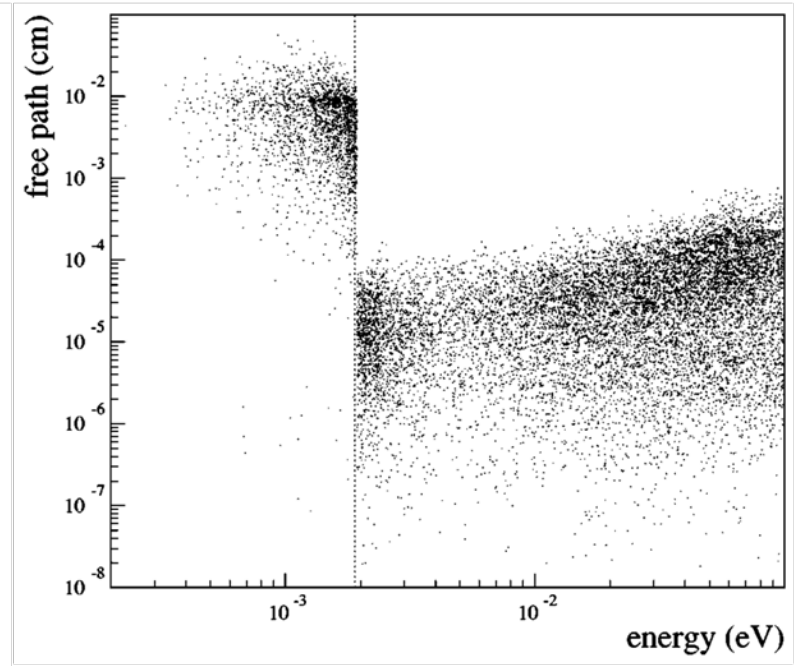

Total cross sections for *p*m(*F*) scattering in 3-K polycrystalline

nH_2 with the fcc structure, for different values of the initial and final muonic atom spin, *F.* The dotted line represents the phonon-annihilation fraction of σ_{11} that results in $p\mu$ energy gain; the sum of contributions from phonon creation and rovibrational excitations to σ_{11}, which lead to $p\mu$ energy loss, is denoted by dash-dotted line. The doubled nuclear scattering cross section σ_{11}^{nuc} for $p\mu\,(F=0)+p$ is shown for comparison (dashed line). Note the Bragg cutoff energy E_B at $\varepsilon \approx 2$ meV for σ_{11}.

Sampled values of the $p\mu$ atom mean free path between consecutive collisions vs the collision energy. A strong increase of the mean free path is seen below the Bragg cutoff energy.

Fusion in pdμ molecule

- The aim of the work is the measurement of the *pdμ* reaction parameters :

$$pd\mu \rightarrow \begin{cases} {}^3He + \mu \\ {}^3He\mu + \gamma \end{cases}$$

The pdμ molecule has two nuclear spin states 1/2 and 3/2 and four total spin states: 0, 1, 1', 2

The present status of the pdμ fusion rates measurements

Parameter	Theory	Experiment				
	J.L Friar, **PRL., 1991**	**L.N. Bogdanova,** **MCF, 1988**	**C. Petitjean,** **MCF, 1990/91**	**G. Griffiths,** **Can. J. Phys., 1963**	**A. Olin,** **Hyp. Int., 1999**	**B. Lauss,** **Hyp. Int., 1999**
$\lambda_{f,\mu}^{1/2}$ [10^6 s^{-1}]	0.062(2)	0.056(6)			0.050 (5)	
$\lambda_{f,\gamma}^{1/2}$ [10^6 s^{-1}]	0.37(1)		0.35(1)		0.376 (15)	
$\lambda_{f,\gamma}^{3/2}$ [10^6 s^{-1}]	0.107(2)		0.11(1)		0.14 (2)	~0.06÷0.09
S_s-factor [eV·b]	0.108(4)			0.12(3)	0.128 (8)	

Experiment

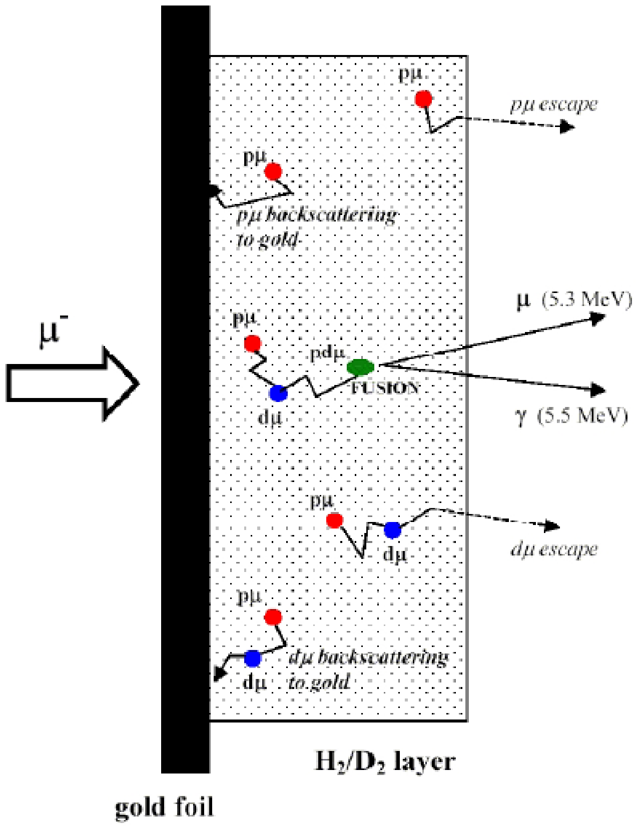

--- 774 *μm*--

Outlook view of the main proceses undergoing in the H_2/D_2 layer:

- muon transfer from $p\mu$ to $d\mu$,
- ***pdμ* formation and fusion with emission muons or gamma,**
- $p\mu$ and $d\mu$ backscattering to the gold foil and
- the $p\mu$ and $d\mu$ atoms diffusion,
- escape of $p\mu$ and $d\mu$ *in* vacuum from the the H_2/D_2 layer.

Kinetic graph

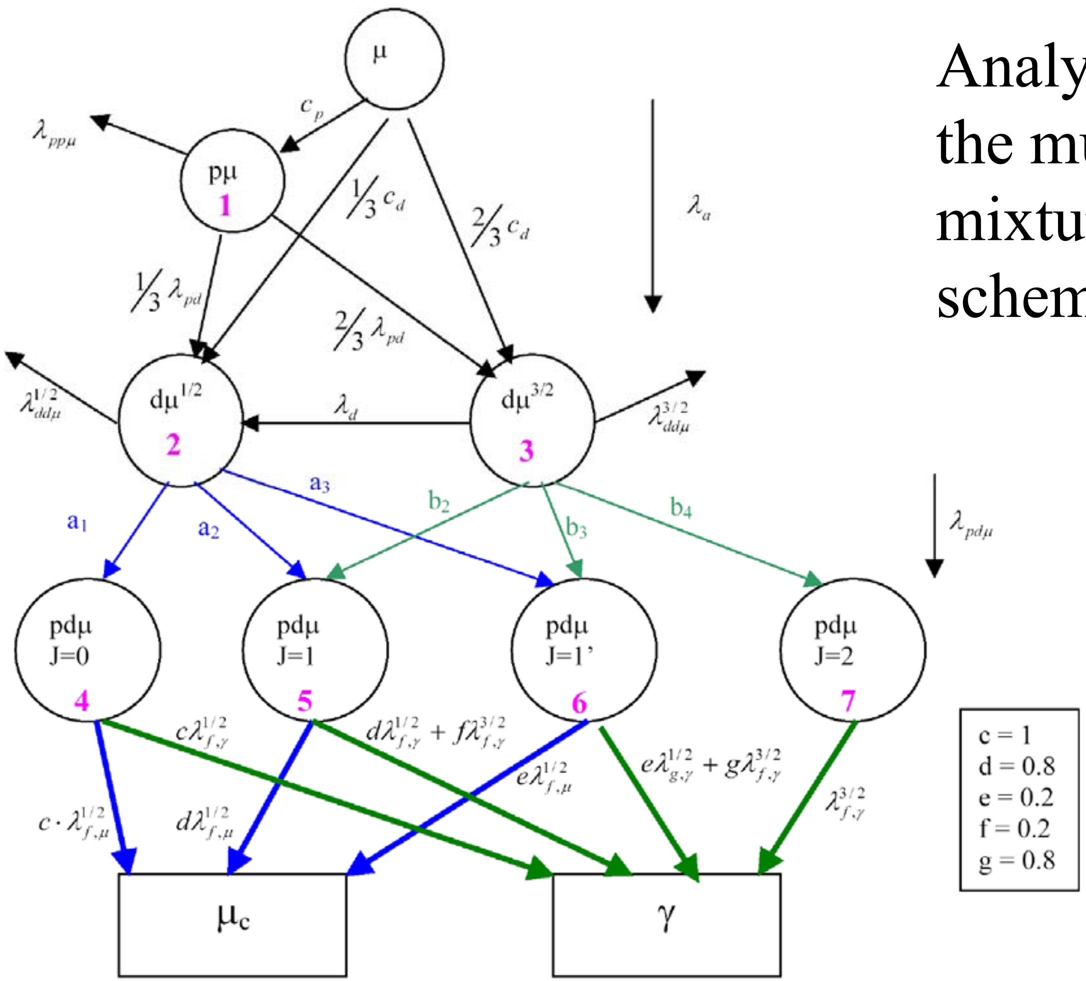

Analytical equations described the muonic processes in H_2/D_2 mixture correspond to present scheme (no muon recycling)

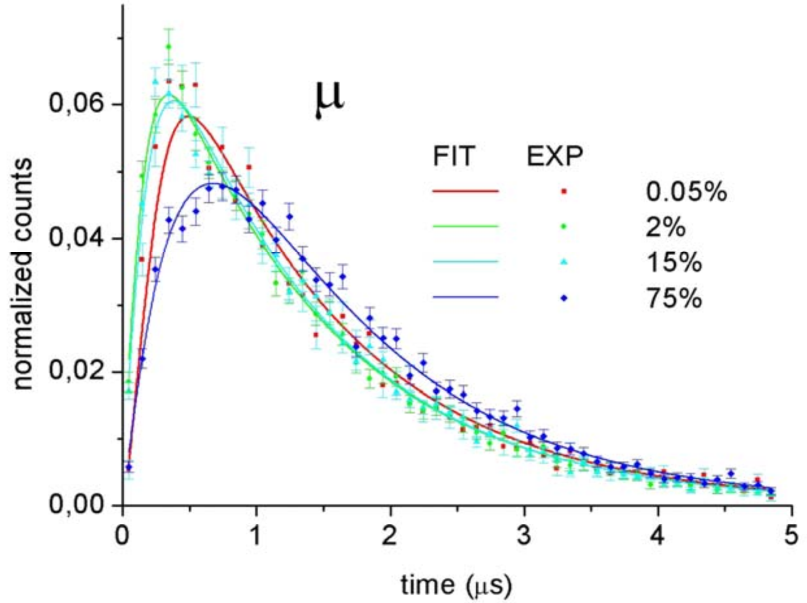

Analitical fitting

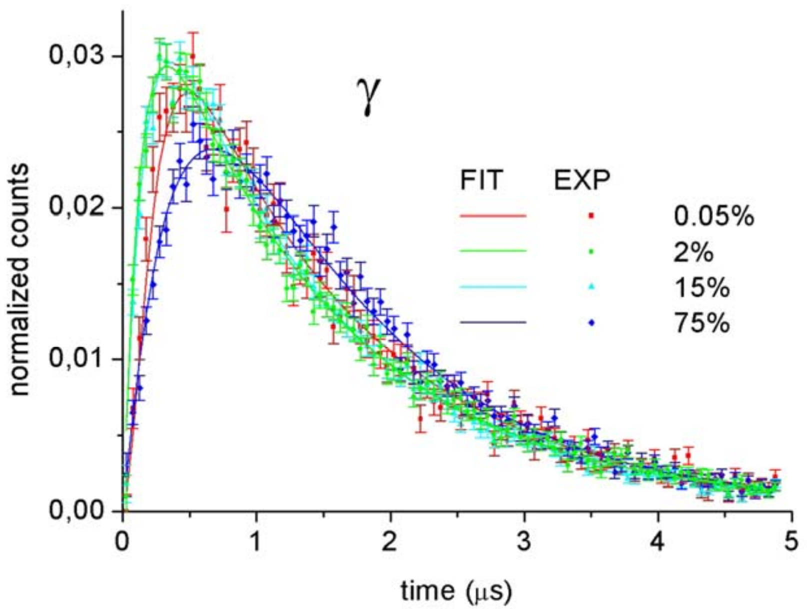

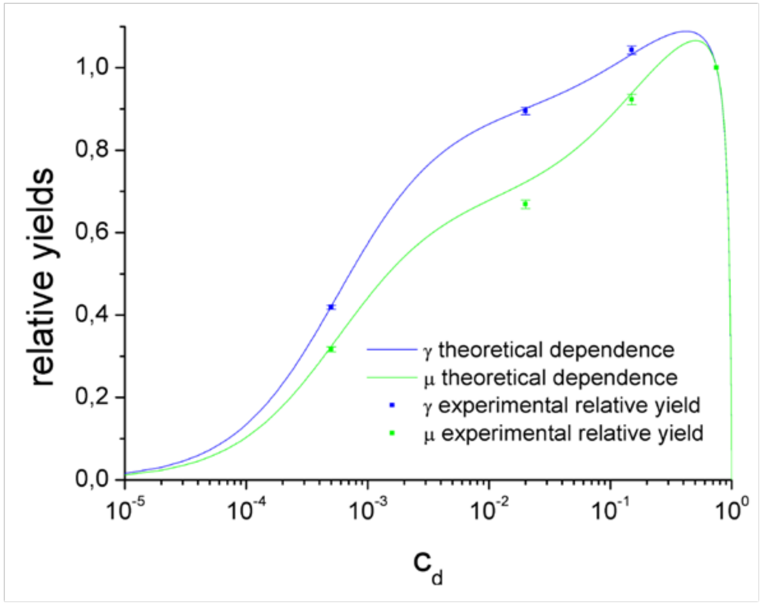

Monte Carlo fitting

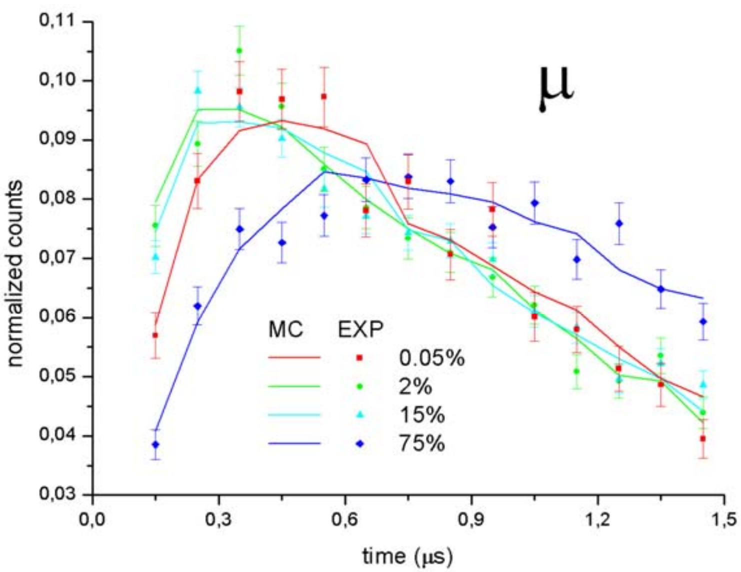

•Simulation of the muon stops in the H/D layer

• Simulation of muonic atoms diffusion processes in the H/D layer

• Simulation of MCF processes occuring during muonic atom diffusion

•Simulation of the muon and muon atoms interaction with the gold foil and the neon layer

• Emission of the *pdμ* fusion γ quanta and conversion muons

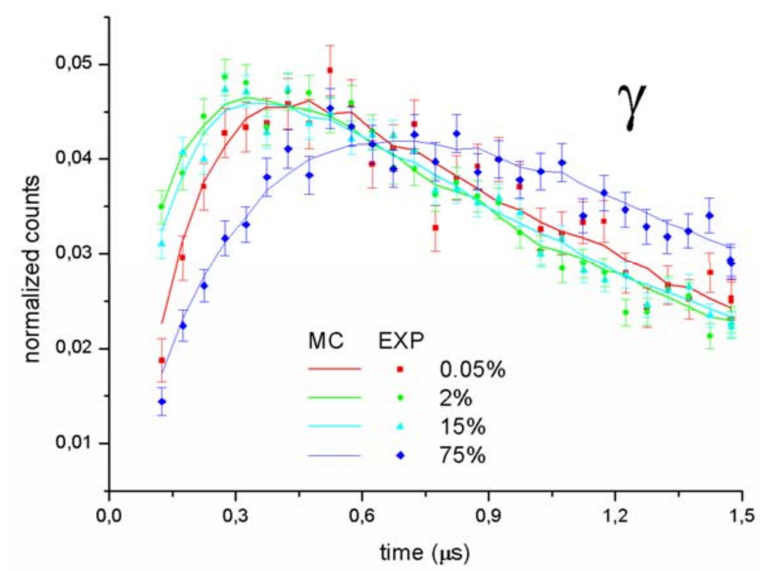

Scalling values for pdμ fusion rate

$$S \in \{0.0, 0.2, 0.4, 0.6, 0.8, 1.0, 1.2, 1.4, 1.6, 1.8, 2.0\}.$$

Results

Parameter	Analitical method $[10^6 \mathrm{s}^{-1}]$	Monte-Carlo method $[10^6 \mathrm{s}^{-1}]$
$\lambda_f^{1/2}$	0.43 ± 0.02	0.42 ± 0.01
$\lambda_{f,\gamma}^{3/2}$	0.08 ± 0.03	0.09 ± 0.02
$\lambda_{f,\gamma}^{1/2}$	0.34 ± 0.04	0.30 ± 0.02
$\lambda_{f,\mu}^{1/2}$	0.09 ± 0.04	0.12 ± 0.02
$\lambda_{pd\mu}$	6.2 ± 0.2	6.7 ± 0.2

S-factor determination

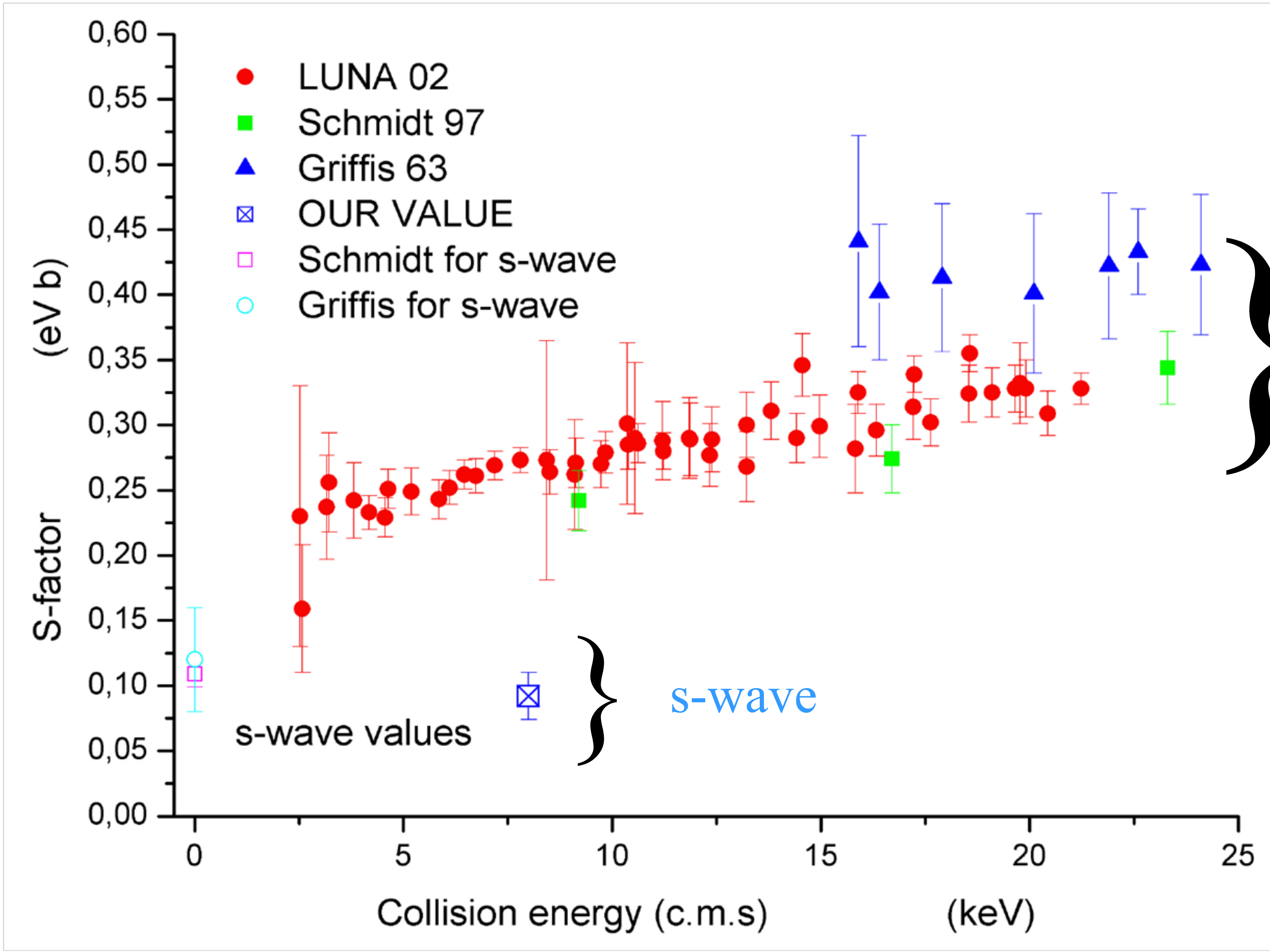

total S-factor s+p wave

Energy distribution of the dμ atoms

at $E_{d\mu} < 0.1$ eV, $\lambda_{d\mu} \approx$ const

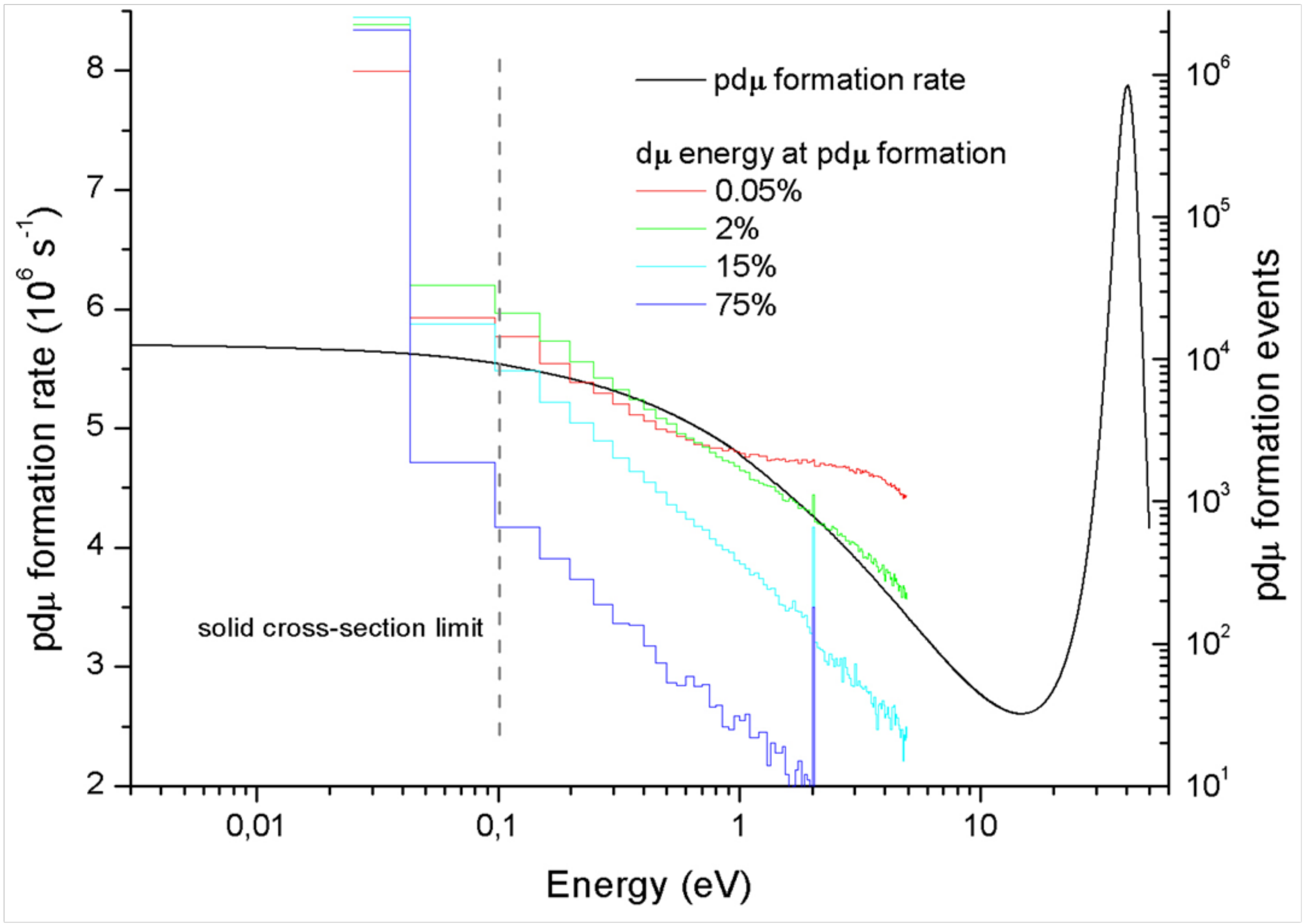

Fraction of dμ with energy less than 0.1 eV:

0.05% - 80%

2% - 93%

15% - 98%

75% - > 99%

(at the moment of pdμ formation)

Time distributions of the pdμ molecules

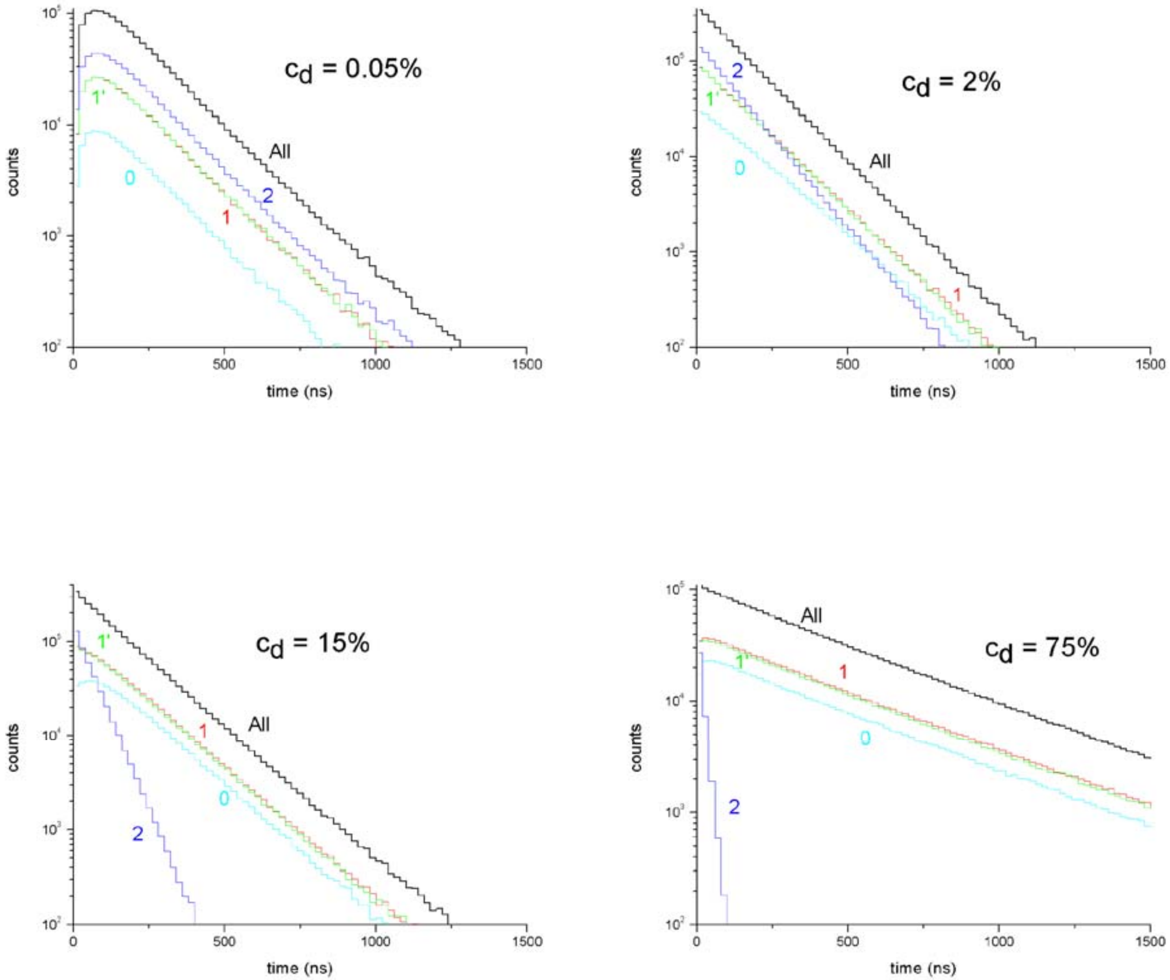

The pdμ time formation distribution for different *J*-states, function $Q^J_{MC}(t)$.

The numbers denote the *J*-state, 'All' represents sum of all particular *J*-curves.

Differential time distribution of the pdμ molecules

$$\frac{dN_{pd\mu}^{J=0}}{dt} = -(\lambda_0 + c \cdot \lambda_f^{1/2}) \cdot N_{pd\mu}^{J=0} + Q_{MC}^{J=0}(t)$$

$$\frac{dN_{pd\mu}^{J=1}}{dt} = -(\lambda_0 + d \cdot \lambda_f^{1/2} + f \cdot \lambda_{f,\gamma}^{3/2}) \cdot N_{pd\mu}^{J=1} + Q_{MC}^{J=1}(t)$$

$$\frac{dN_{pd\mu}^{J=1'}}{dt} = -(\lambda_0 + e \cdot \lambda_f^{1/2} + g \cdot \lambda_{f,\gamma}^{3/2}) \cdot N_{pd\mu}^{J=1'} + Q_{MC}^{J=1'}(t)$$

$$\frac{dN_{pd\mu}^{J=2}}{dt} = -(\lambda_0 + \lambda_{f,\gamma}^{3/2}) \cdot N_{pd\mu}^{J=2} + Q_{MC}^{J=2}(t)$$

$$\begin{aligned}\frac{dN_\mu}{dt} &= c \cdot \lambda_{f,\mu}^{1/2} \cdot N_{pd\mu}^{J=0} + d \cdot \lambda_{f,\mu}^{1/2} \cdot N_{pd\mu}^{J=1} + e \cdot \lambda_{f,\mu}^{1/2} \cdot N_{pd\mu}^{J=1'} = \\ &\lambda_{f,\mu}^{1/2} \cdot \left(c \cdot N_{pd\mu}^{J=0} + d \cdot N_{pd\mu}^{J=1} + e \cdot N_{pd\mu}^{J=1'}\right)\end{aligned} \qquad (19)$$

$$\begin{aligned}\frac{dN_\gamma}{dt} &= c \cdot \lambda_{f,\gamma}^{1/2} \cdot N_{pd\mu}^{J=0} + (d \cdot \lambda_{f,\gamma}^{1/2} + f \cdot \lambda_{f,\gamma}^{3/2}) \cdot N_{pd\mu}^{J=1} + (e \cdot \lambda_{f,\gamma}^{1/2} + g \cdot \lambda_{f,\gamma}^{3/2}) \cdot N_{pd\mu}^{J=1'} + \lambda_{f,\gamma}^{3/2} \cdot N_{pd\mu}^{J=2} = \\ &\lambda_{f,\gamma}^{1/2} \cdot \left(c \cdot N_{pd\mu}^{J=0} + d \cdot N_{pd\mu}^{J=1} + e \cdot N_{pd\mu}^{J=1'}\right) + \lambda_{f,\gamma}^{3/2} \cdot \left(f \cdot N_{pd\mu}^{J=1} + g \cdot N_{pd\mu}^{J=1'} + N_{pd\mu}^{J=2}\right)\end{aligned} \qquad (20)$$

pdμ fusion partial rates

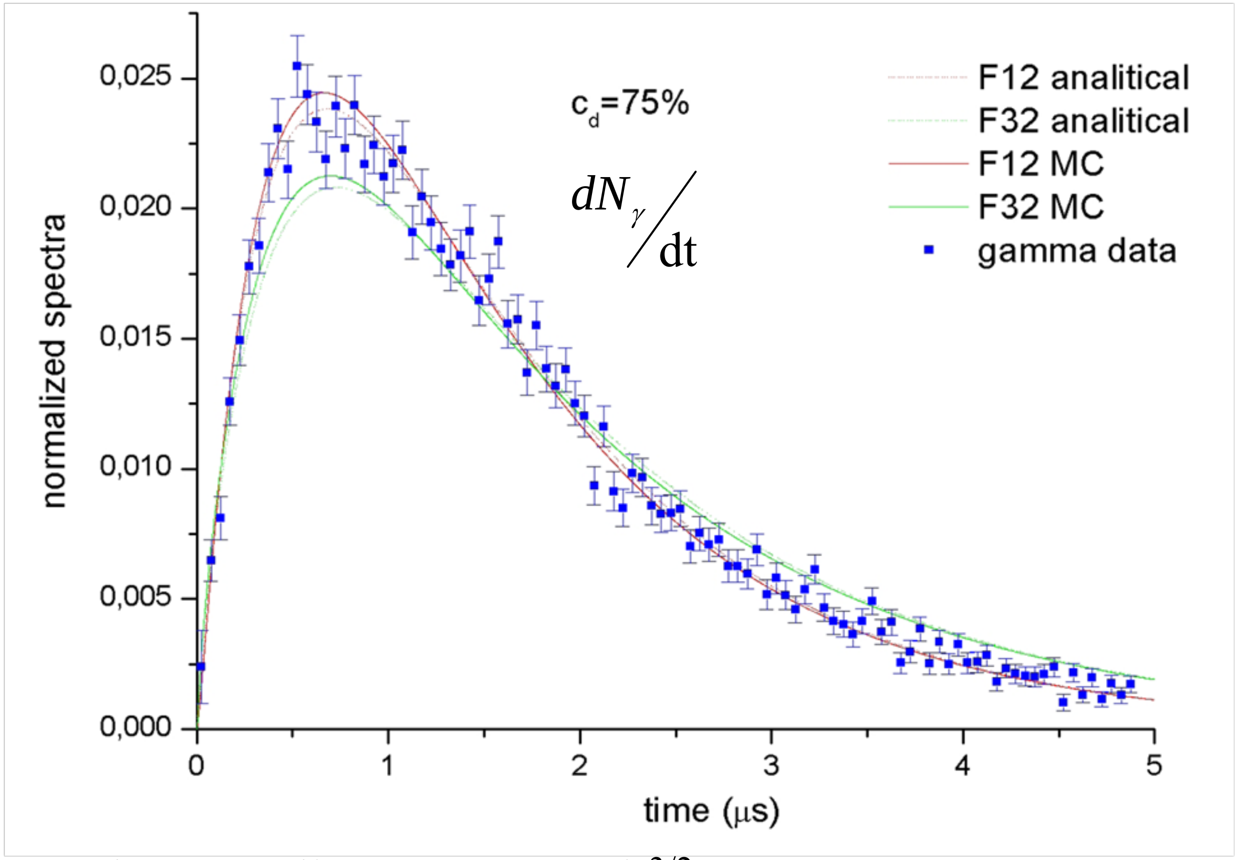

$$\frac{dN_\mu}{dt} = \lambda_{f,\mu}^{1/2} \cdot F_{1/2}$$

$$\frac{dN_\gamma}{dt} = \lambda_{f,\gamma}^{1/2} \cdot F_{1/2} + \lambda_{f,\gamma}^{3/2} \cdot F_{3/2}$$

Rewriten equations from previous page

Only green line – $\lambda^{3/2}=0$

Only red line - $\lambda^{1/2}=0$

It is impossible to determine the fusion partial rates with high accuracy using our experimental data

Emission of pμ and dμ atoms

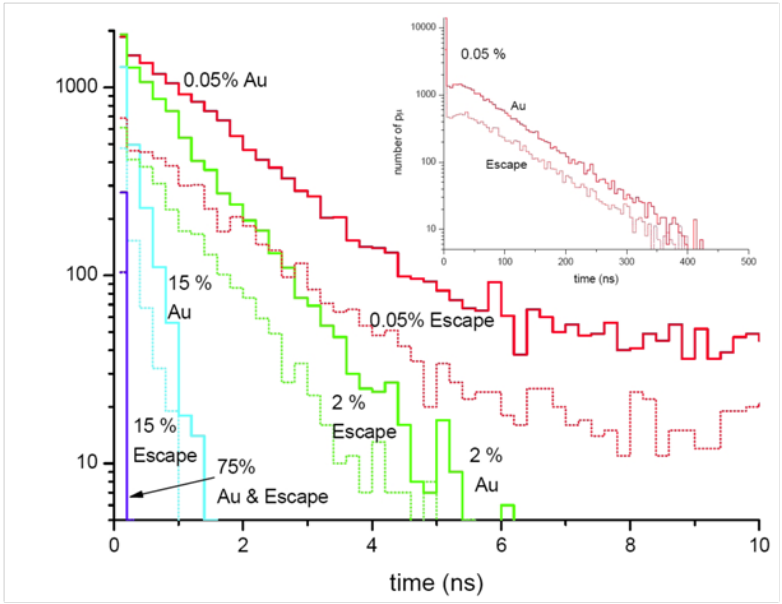

- backscattering of $p\mu$ and escape of $p\mu$ from H_2/D_2 layer, picture in upper right corner shows $p\mu$ for 0.05% for long time scale

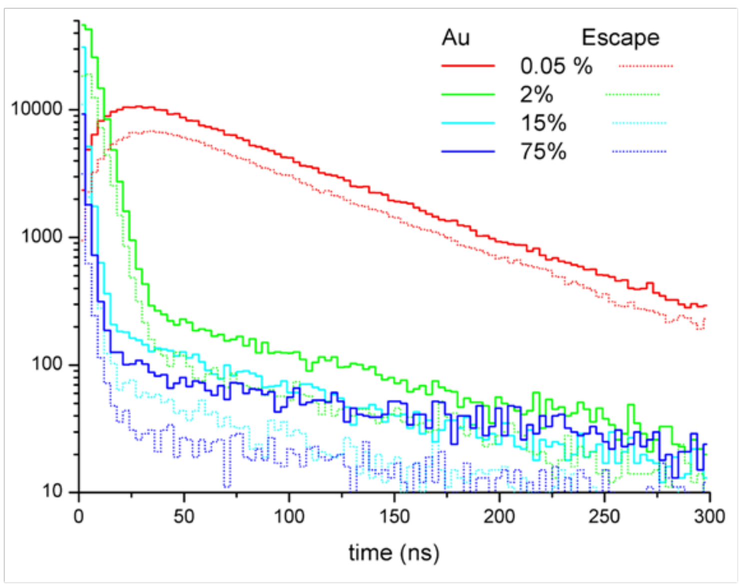

- $d\mu$ backscattering to the gold foil and escape $d\mu$ from H_2/D_2 layer

PSI experiment

Aim:

- Study of the nuclear fusion in a muonic $d\mu^3He$ complex

Collaboration:

- JINR,
- University of Fribourg (Switzerland),
- PSI (Switzerland),
- University of Science and Technology (Poland),
- Munich University (Germany).

Scheme muonic processes in $D_2/^3He$ mixture

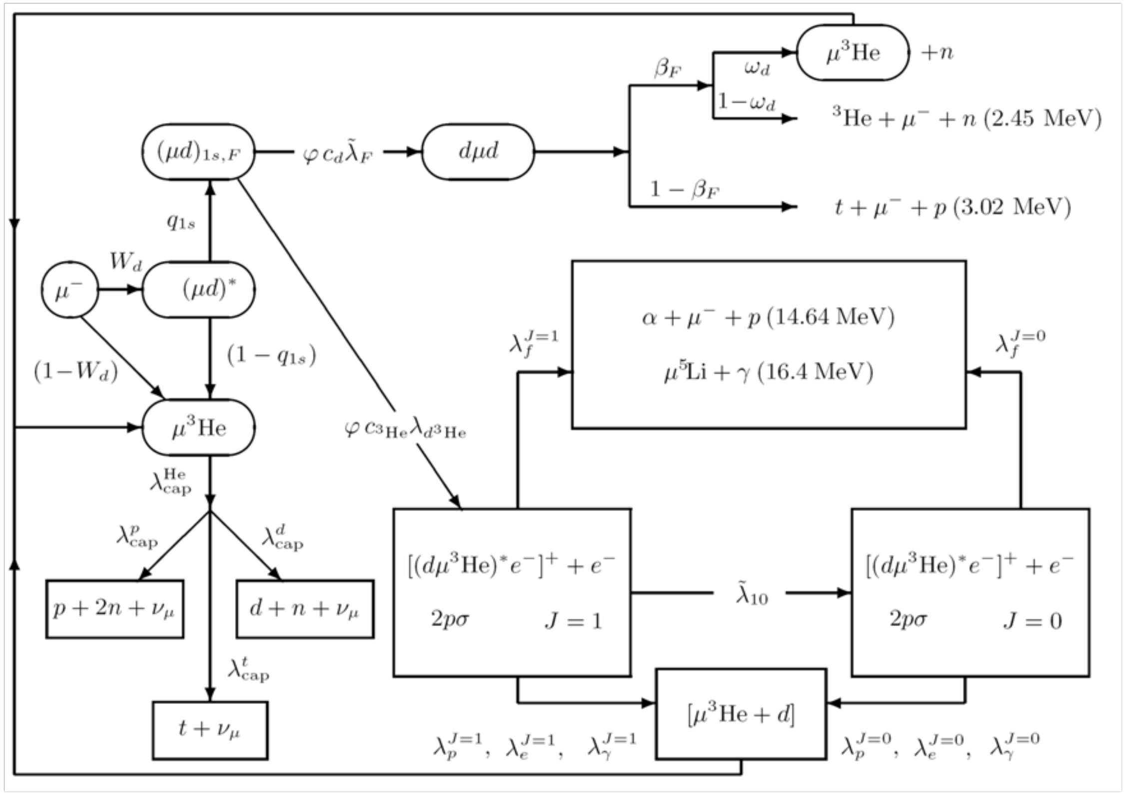

$$Y_p(t_1,t_2) = Y_p^1(t_1,t_2) + Y_p^0(t_1,t_2) = N_\mu^{D/He} \frac{\tilde{\lambda}_f}{\lambda_\Sigma} \frac{\varphi c_{^3He} \lambda_{d^3He} W_d q_{1s} \varepsilon_Y \varepsilon_p}{\lambda_{d\mu}},$$

$$\lambda_{d\mu} = \lambda_0 + \varphi c_{^3He} \lambda_{d^3He} + \varphi c_d \tilde{\lambda}_F \left[1 - W_d q_{1s}(1-\beta_F \omega_d)\right].$$

$$\tilde{\lambda}_f = \left(\lambda_f^{J=1} \frac{\lambda_\Sigma^0}{\tilde{\lambda}_{10} + \lambda_\Sigma^0} + \lambda_f^{J=0} \frac{\tilde{\lambda}_{10}}{\tilde{\lambda}_{10} + \lambda_\Sigma^0}\right),$$

$$\lambda_\Sigma = \lambda_\Sigma^0 \left(\frac{\tilde{\lambda}_{10} + \lambda_\Sigma^1}{\tilde{\lambda}_{10} + \lambda_\Sigma^0}\right).$$

$$\tilde{\lambda}_f = \frac{Y_p(t_1,t_2) \lambda_{d\mu} \lambda_\Sigma}{N_\mu^{D/He} W_d q_{1s} \varphi c_{^3He} \lambda_{d^3He} \varepsilon_p \varepsilon_e \varepsilon_t \varepsilon_Y},$$

$$\frac{dN^1_{d\mu^3He}}{dt} = +\varphi c_{^3He} \lambda_{d^3He} N_{d\mu} - \lambda_\Sigma^1 N^1_{d\mu^3He}$$

$$\frac{dN^0_{d\mu^3He}}{dt} = +\tilde{\lambda}_{10} N^1_{d\mu^3He} - \lambda_\Sigma^0 N^0_{d\mu^3He}$$

$$\lambda_\Sigma^1 = \left(\lambda_0 + \lambda_p^{J=1} + \lambda_\gamma^{J=1} + \lambda_e^{J=1} + \lambda_f^{J=1} + \tilde{\lambda}_{10}\right)$$

$$\lambda_\Sigma^0 = \left(\lambda_0 + \lambda_p^{J=0} + \lambda_\gamma^{J=0} + \lambda_e^{J=0} + \lambda_f^{J=0}\right),$$

Experimental set-up

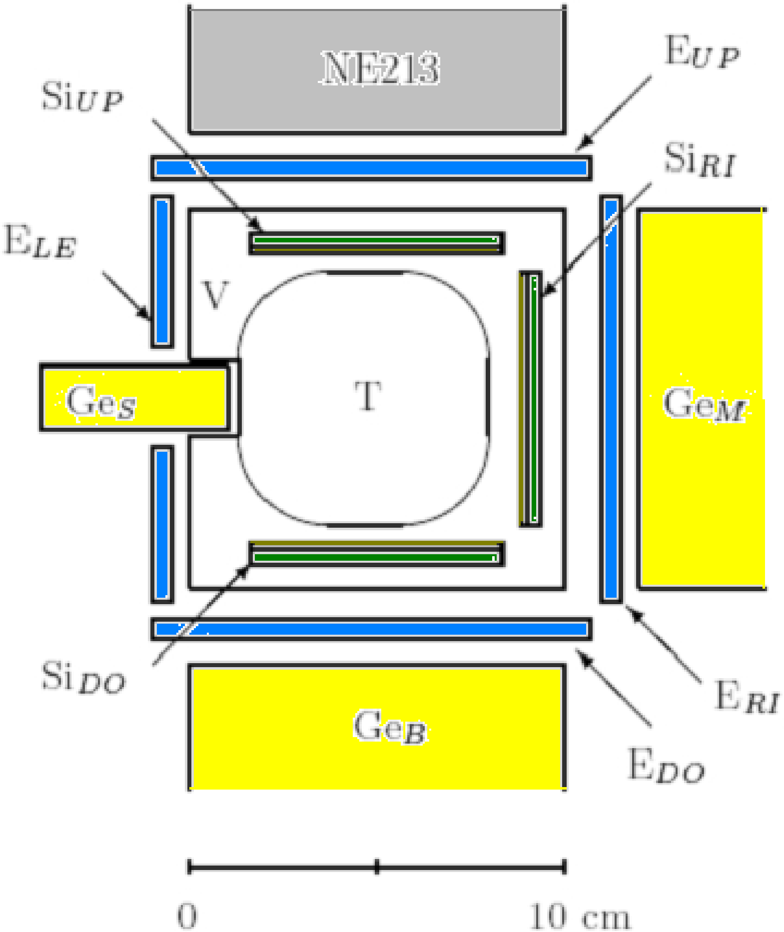

A gaeous criogenic target-criostat was developed in Dubna, designed to work in the ~30 K temperature, the system of purifing and filling the target with pure hydrogen and helium, and also the registration system of the protons with energy 14.64 MeV

Si (E) detectors, Si (dE) detectors

Muon decay electrons

6.85 KeV X rays detectors

2.5 MeV neutrons

Scheme of the experimental set-up, view in muon fly direction

Experimental conditions

Experimental conditions for the D_2 + ^3He mixtures with an atomic concentration of helium c_{3He} = 0.0496.

N_μ is the number of muons stopped in our apparatus.

Run	P_μ [MeV/c]	T [K]	p [kPa]	φ [LHD]	N_μ [10^9]
I	34.0	32.8	513.0	0.0585	8.875
II	38.0	34.5	1224.4	0.1680	3.928

Two-dimensional event distribution detected by the Si(dE-E) telescopes

No coincidence with muon decay electrons

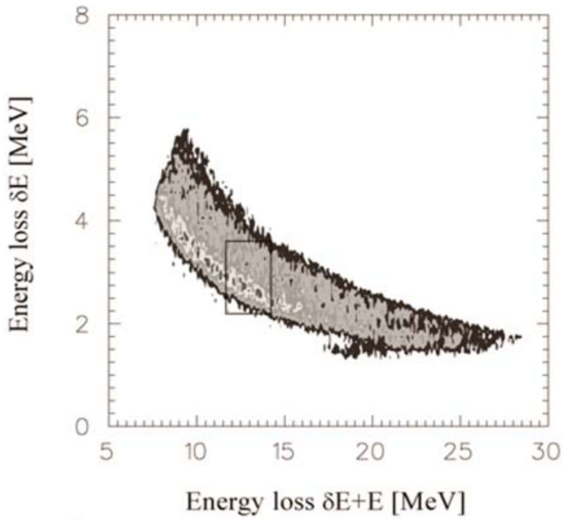

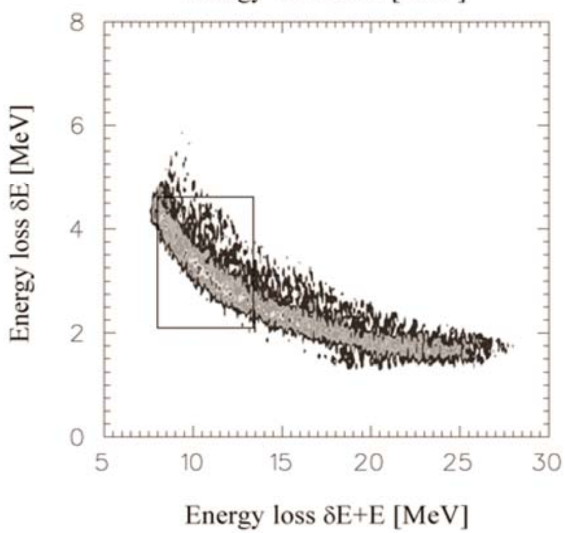

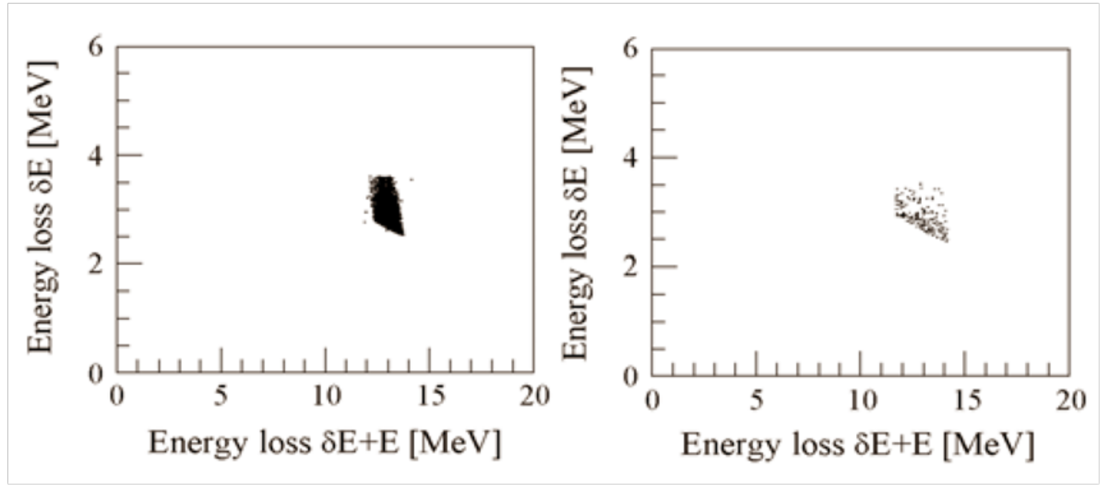

Two-dimensional distributions of Si(dE − (dE + E)) events obtained in run I by the Monte Carlo method and corresponding to the detection of protons from reactions:

$d\mu^3He \rightarrow \alpha + \mu + p \; (14.64\text{MeV})$

and

$$d\mu + d \rightarrow dd\mu \rightarrow {}^3He \; (0.8\,\text{MeV}) + n$$
$$+$$
$$d \rightarrow \alpha + p \; (14.64\,\text{MeV})$$

within the time interval Δt_{Si}.

Two-dimensional event distributions detected by the Si(*dE* − *E*) telescopes in runs I (top) and II (down). The rectangles indicate the energy regions corresponding to the values of *δE* and ΔE_{Σ} as found via MC.

Background

Two-dimensional Si($dE-E$) telescope event distributions for a run with:

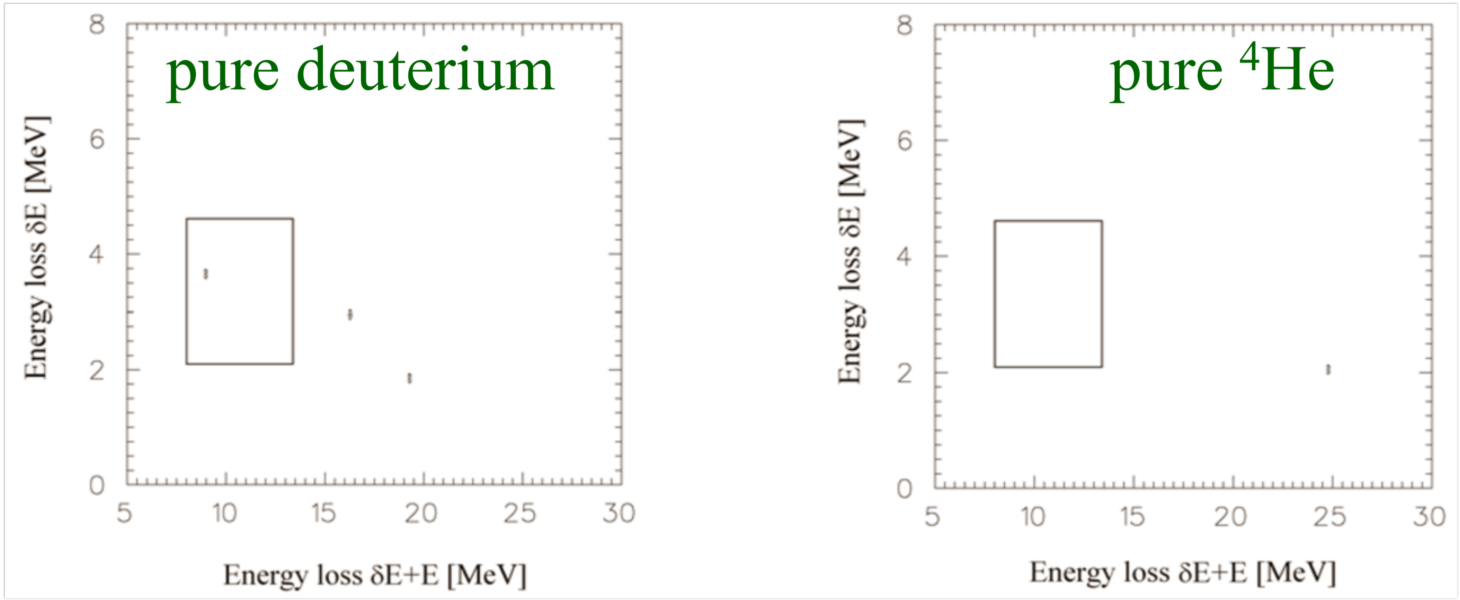

the del-*e* coincidences and within the Δt_{Si} interval.

The rectangle is the region corresponding to the chosen energy intervals δE and ΔE_{Σ} for detection events from dμ^3He fusion in the run with the D_2 +^{3}He mixture at φ = 0.168.

	Region A		Region B		Region C	
Run	ΔE_{Σ}	δE	ΔE_{Σ}	δE	ΔE_{Σ}	δE
I	0–11.7	3.6–6	0–11.7	0–3.6	14.2–25	1.8–6
II	0–8	4.6–6	0–8	0–4.6	13.6–25	1.5–6

The three regions dividing the two-dimensional ($\delta E-\Delta E_{\Sigma}$) distributions as used for the background studies. All energies are given in MeV.

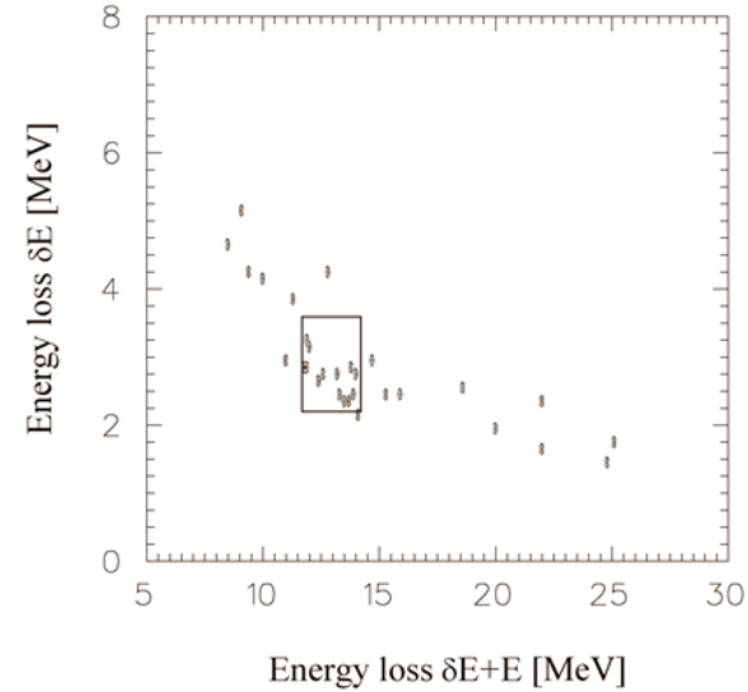

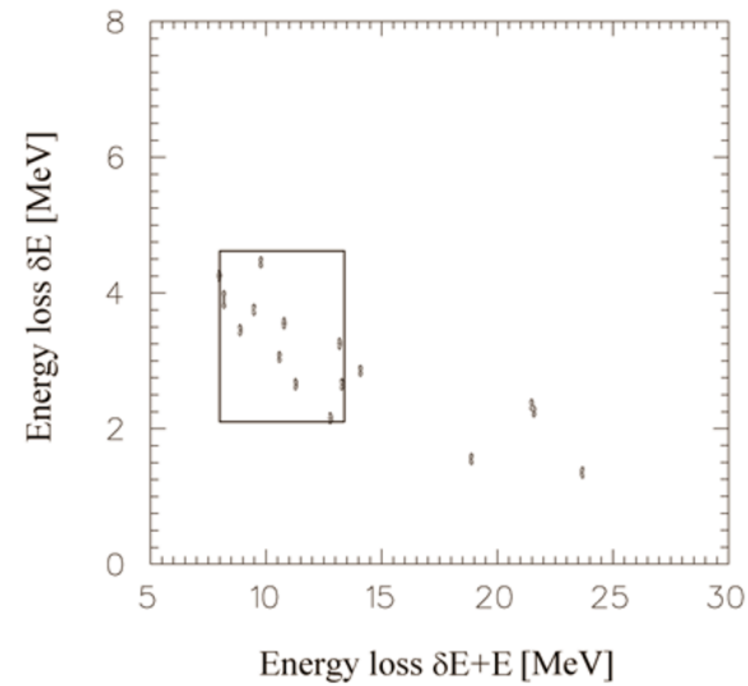

Observation of the fusion events

Two-dimensional Si(*dE−E*) telescope event distributions for runs I (top) and II (down) with the del-e coincidence and the time

Δt_{Si} (run I): $0.7 \le t_{\mathrm{Si}} \le 2.2\ \mu s$

Δt_{Si} (run II): $0.4 \le t_{\mathrm{Si}} \le 1.2\ \mu s$.

$\Delta E_{\Sigma} = [11.7\text{–}14.2]$ MeV for run I and $\Delta E_{\Sigma} = [8.0\text{–}13.4]$ MeV for run II.

After backgroung substraction:

$$Y_p = 7.7^{+4.4}_{-3.4} \qquad \text{run I}$$

$$Y_p = 7.5^{+3.8}_{-3.2} \qquad \text{run II.}$$

Results:

Run	$\tilde{\lambda}_{10}$ $[10^{11}\ s^{-1}]$	$\lambda_f^{J=0}$ $[10^5\ s^{-1}]$	$\tilde{\lambda}_f$ $[10^5\ s^{-1}]$	λ_{Σ} $[10^{11}\ s^{-1}]$
I	5.2	$9.7^{+5.7}_{-2.6}$	$4.5^{+2.6}_{-2.0}$	6.54
II	7.5	$12.4^{+6.5}_{-5.4}$	$6.9^{+3.6}_{-3.0}$	6.44

Muon capture by ^{3}He nuclei

$$\mu^- + {}^3\text{He} \rightarrow p + n + n + \nu_\mu \qquad \mu^- + {}^3\text{He} \rightarrow d + n + \nu_\mu$$

Two methods of the data analysis:

- **(I) Least square:** reproduce the experimental data and to minimize the free parameters which are required by such a simulation.

- **(II) Bayes theorem:** to determine the initial energy distribution of the protons and the deuterons produced by muon capture

Method	I	(s^{-1})	II
$\lambda^p_{cap}(10 \leqslant E_p \leqslant 49\ \text{MeV})$	36.7 ± 1.2		36.8 ± 0.8
$\lambda^d_{cap}(13 \leqslant E_p \leqslant 31\ \text{MeV})$	21.3 ± 1.6		21.9 ± 0.6

Muon capture results – differential rates

$d\lambda^{p}_{\text{cap}}(E_p)/dE_p$

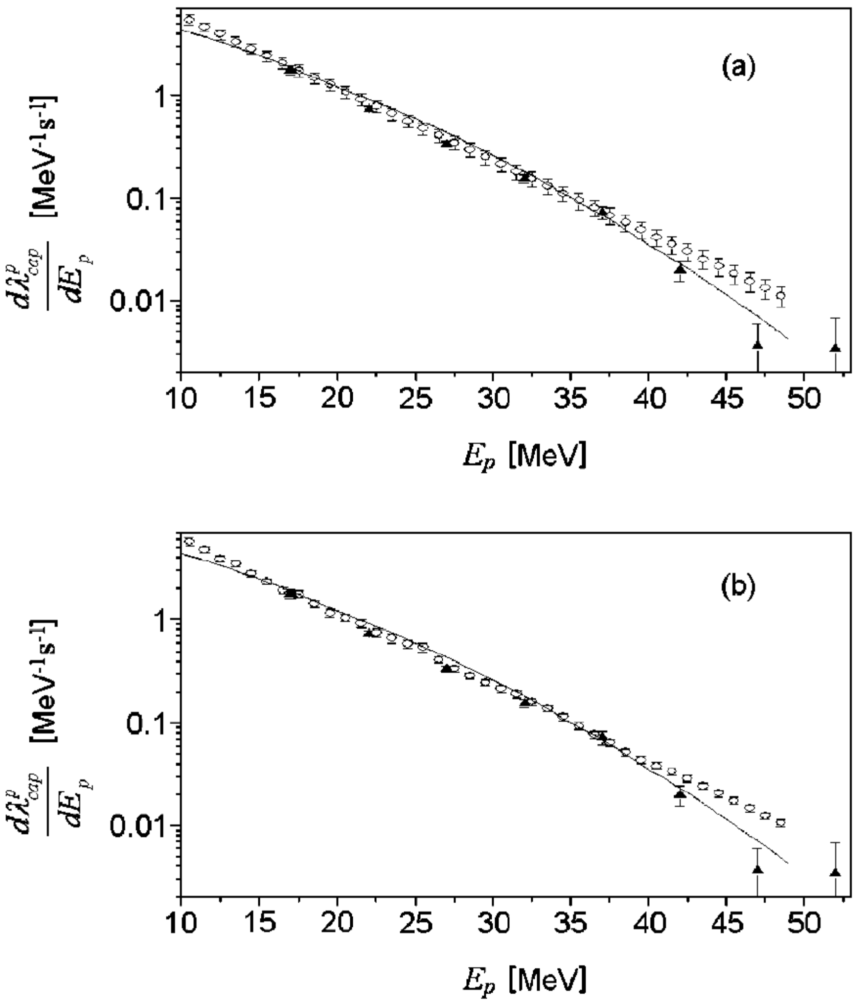

Differential rates (open circles) found by methods I (a) and II)(b) averaged over runs (I–III). Black triangles are the results of S.E. Kuhn et al., W.J. Cummings et al.; the solid line corresponds to the model of A.C. Philips et al..

$d\lambda^{d}_{\text{cap}}(E_d)/dE_d$

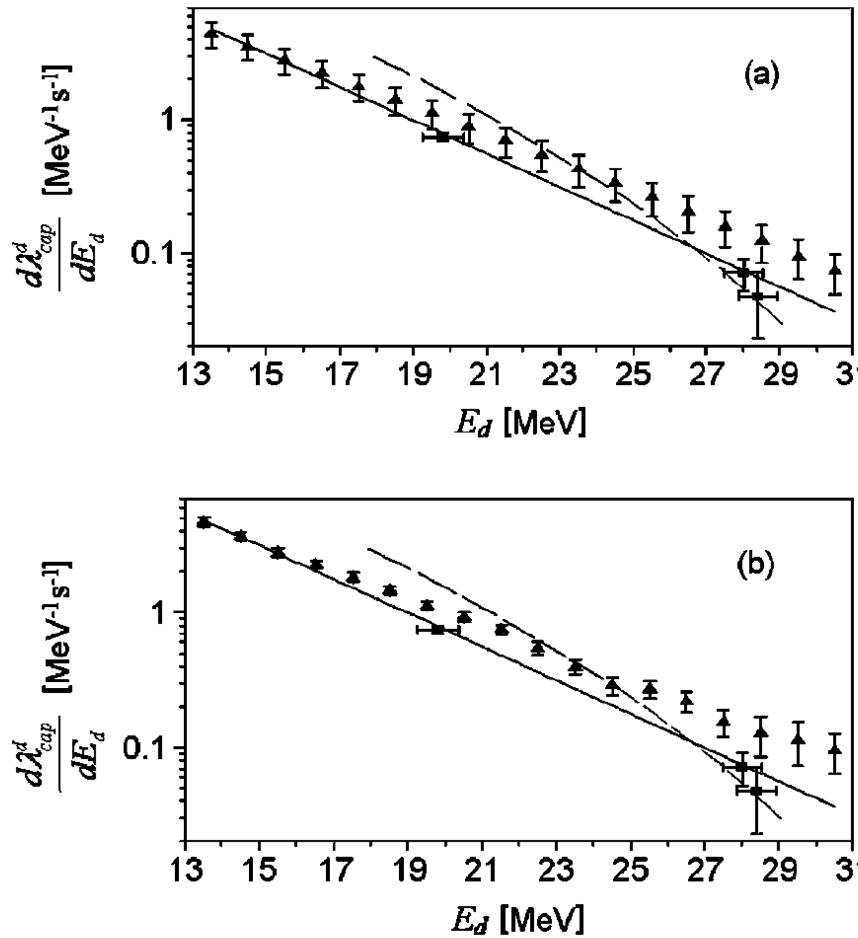

Differential rates (black triangles) found by methods I (a) and II (b) and averaged over runs (I–III). Black boxes are the results of S.E. Kuhn et al., W.J. Cummings et al.; the solid line corresponds to the model of of A.C. Philips et al.; the dotted line is based on calculations from R. Skibinski et al..

Relative probabilities of the radiative decay

For the first time the relative probabilities of the radiative decay of the $d\mu^3He$ complex for the two densities (D_2 + ^3He) mixture ere measured:

$k_{d\mu 3He} = 0.203 \pm 0.014$ ($\varphi = 0.0585$),

$k_{d\mu 3He} = 0.228 \pm 0.012$ ($\varphi = 0.168$).

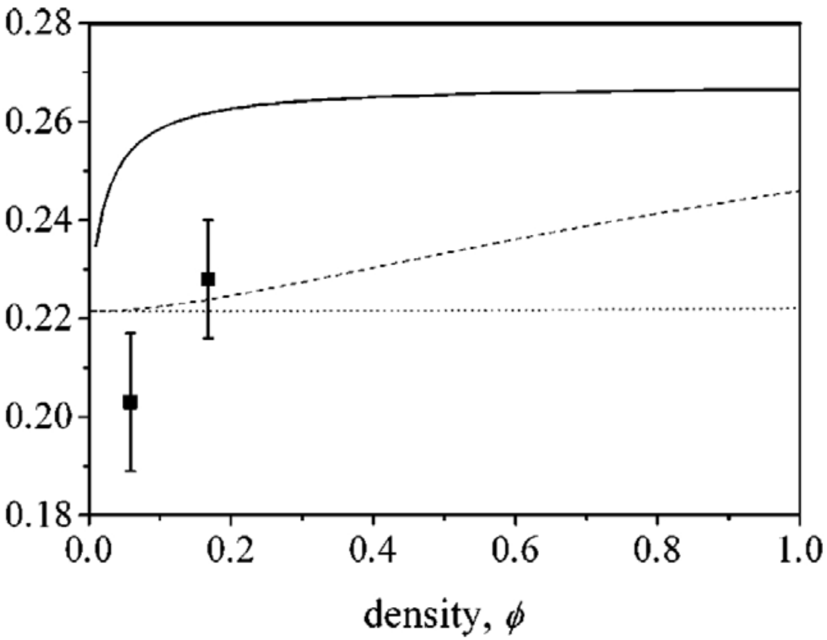

The dependence of the probability of radiational decay $k_{d\mu 3He}$ from density. Points with experimental errors are the values from the experiment. The solid line is for mechanism (2) for value $\lambda_{Aug}{}^{int} = 10^{12}\ s^{-1}$, the dashed lines are for mechanism (1), and: dashed line is for $\lambda_{Aug}{}^{ext} = 8.5\ 10^{11}\ s^{-1}$, and dotted line for $\lambda_{Aug}{}^{ext} = 8.5\ 10^{11}\ s^{-1}$.

1 → 0 transfer

Mechanism (1) and (2):

$$d\mu + {}^3\mathrm{He} \rightarrow \left[(d\mu{}^3\mathrm{He})^{2+}_{2p\sigma,J=1}e\right]^+ + e$$

Mechanism (1):

$$\left[(d\mu{}^3\mathrm{He})^{2+}_{2p\sigma,J=1}e\right]^+ + \mathrm{He} \xrightarrow{\lambda_n} \left[(d\mu{}^3\mathrm{He})^{2+}_{2p\sigma,J=1}2e\right] + \mathrm{He}^+$$

$$\left[(d\mu{}^3\mathrm{He})^{2+}_{2p\sigma,J=1}2e\right] + \mathrm{D(D_2)} \xrightarrow{\lambda^{ext}_{Aug}} \left[(d\mu{}^3\mathrm{He})^{2+}_{2p\sigma,J=0}2e\right] + \mathrm{D^+(D_2^+)} + e.$$

Mechanism (2):

$$\left[(d\mu{}^3\mathrm{He})^{2+}_{2p\sigma,J=1}e\right]^+ + \mathrm{D_2} \xrightarrow{\lambda_{cl}} \left[(d\mu{}^3\mathrm{He})^{2+}_{2p\sigma,J=0}e\right]\mathrm{D_2}$$

$$\left[(d\mu{}^3\mathrm{He})^{2+}_{2p\sigma,J=1}e\right]\mathrm{D_2} \xrightarrow{\lambda^{inn}_{Aug}} \left[(d\mu{}^3\mathrm{He})^{2+}_{2p\sigma,J=0}e\right]\mathrm{D_2^+} + e$$

The q_{1s} coefficient

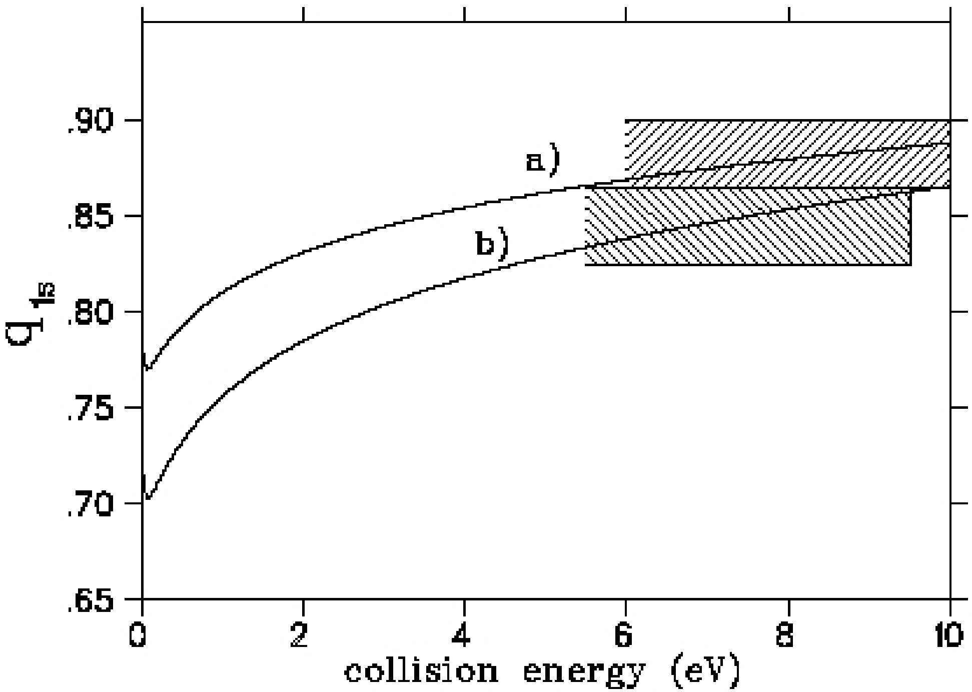

The q_{1s} probaility of the dμ-atom, formated in the excited state, reach the ground level 1s

The theoretical value q_{1s} coefficient dependence from energy calculated for the exposition I (curve a) and for the exposition II (curve b). Experimental values are equal 0.882 ± 0.018 and 0.844 ± 0.020, respectively.

Filled areas show region of measured values of the q_{1s}

Main results

- First observation of the fusion in $d\mu^3He$ and measurement of the fusion rate and rate from J=0
- Measurement of the $d\mu^3He$ radiative decay branching ratio

The following parameters were determined

- Formation rate of the $d\mu^3He$
- Q_{1s} coefficient
- Relative intensities of the prompt and delayed K series
- Muon capture by ^3He with proton and deuteron emission
- Differential probabilities of the muon capture
- Stopping power in helium-deuterium mixtures

Publication results

[1] V.M.Bystritsky et al., PSI Proposal R-98-02, Measurement of nuclear fusion reactions in mudHe3-molecules, PSI, 1998; Scientific Report PSI, Volume 1, 1998.

[2] V.F.Boreiko, V.M.Bystritsky et al, New target cryostat for experiments with negative muons, NIM A 416 (1998) 221.

[3] V.M. Bystritsky et al., Method of investigation of nuclear reactions in charge-nonsymmetrical complexes, NIM A 432 (1999) 188-194.

[4] A. Del Rosso,... V.M. Bystritsky et al., Measurement of the fusion rate in μd^3He, Hyp. Interactions 118 (1999) 177-182.

[5] V.M. Bystritsky et al., Medium density variation as a method for investigating properties of meso-molecular resonances, Hyp. Intreraction 119 (1999) 369-371.

[6] V.A. Stolupin,...V.M. Bystritsky et al., A cryogenic target to study charge nonsymmetric muonic molecules, Hyp. Intreraction 119 (1999) 373-375.

[7] P.Knowles,... V.M. Bystritsky et al., Experimental search for μd^3He fusion, Hyp. Interaction 138 (2002) 289-294.

[8] V.M. Bystritsky et al., Dynamics of muonic atom cascade in hydrogen-helium mixtures, European Phys. Journal D 5 (1998) 185.

[9] V.M. Bystritsky et al., Muonic atom cascade processes in the mixture of hydrogen and helium isotopes, Kerntechnik 64 (1999) 294.

[10] V.M. Bystritsky et al., Method for Experimentally Determining the Features of Nuclear Fusion from mu-Molecular Resonance States, Physics of Atomic Nuclei 62 (1999) 281.

[11] V.M. Bystritsky et al., Time evalution of cascade processes of muonic atoms in hydrogen-helium mixtures, European Phys. Journal D 8 (1999) 75-83.

[12] V.M. Bystritsky et al., Muon capture by 3He nuclei followed by proton and deuteron production, Phys. Rev. A 69 (2004) 012712.

[13] V.M. Bystritsky et al., Experimental study of μ-atomic and μ-molecular processes in pure helium and deuterium-helium mixtures, Phys. Rev. A 71(2005) 032723.

[14] V.M. Bystritsky et al., Nuclear fusion in muonic deuterium-helium complex, Preprint JINR, E 15-2005-91, Dubna, (2005); to be published in European Phys. Journal (2005).

[15] F. Mulhauser, .. V.M. Bystritsky et al., Ramsauer-Townsend effect in muonic atom scattering, to be published in Phys. Rev. Lett.(2006).

Conclusion

The results obtained in the experiments in TRIUMF and PSI essentially widened understanding of the complicated scheme of the mu-atomic and mu-molecular processes occuring in the solid hydrogen isotopes mixturies and gaseous hydrogen-helium mixturies